STRANGENESS PRODUCTION WITH PROTONS AND PIONS

Carl B. Dover

Physics Department
Brookhaven National Laboratory
Upton, New York 11973

ABSTRACT

We discuss the spectrum of physics questions related to strangeness which could be addressed with intense beams of protons and pions in the few GeV region. We focus on various aspects of strangeness production, including hyperon production in pp collisions, studies of hyperon–nucleon scattering, production of hypernuclei in proton and pion–nucleus collisions, and spin phenomena in hypernuclei.

STRANGENESS PRODUCTION
WITH PROTONS AND PIONS

Carl B. Dover

Physics Department
Brookhaven National Laboratory
Upton, New York 11973

ABSTRACT

We discuss the spectrum of physics questions related to strangeness which could be addressed with intense beams of protons and pions in the few GeV region. We focus on various aspects of strangeness production, including hyperon production in pp collisions, studies of hyperon–nucleon scattering, production of hypernuclei in proton and pion–nucleus collisions, and spin phenomena in hypernuclei.

1. Introduction and Motivation

Nucleon–nucleon (NN) interactions in the multi–GeV energy range produce a number of final states. Most often pions are produced, but also strange particles emerge from such collisions, for instance Λ, Σ or Ξ baryons, or kaons ($K^{\pm}$, K_L, K_S). In the present talk, we emphasize the various aspects of the strangeness production mechanism, as well as the study of secondary hyperon–nucleon collisions as a means of shedding light on the SU(3) structure of baryon-baryon interactions. We also consider the production of hypernuclei (Λ bound to a nuclear core) in proton-nucleus (pA) collisions, and via the (π, K) associated production reaction.

This paper is organized as follows: In Section 2, we review the existing data on strangeness production in pp collisions, focusing on the $\Lambda p K^+$ and $\Sigma N K^+$ final states. In Section 3, the status of our knowledge of low energy hyperon–nucleon (YN) scattering is reviewed, with an emphasis on the spin dependence of the interaction and tests of SU(3) symmetry. The formation of hyperfragments ($_\Lambda A$) in pA collisions is examined in Section 4. Some comments on hypernuclear production with pion beams is given in Section 5, emphasizing polarization phenomena.

2. Strangeness Production in pp Collisions

The lowest–lying threshold for strangeness production in pp collisions corresponds to a lab momentum $p_L = 2.34$ GeV/c for the reaction $pp \rightarrow \Lambda pK^+$. As p_L rises above threshold, the total cross section for the $pp \rightarrow \Lambda pK^+$ reaction first rises rapidly, attains a peak of 50–60 μb near 5–6 GeV/c, and then drops off slowly. The inclusive cross section for Λ production, on the other hand, continues to rise, attaining values of 4–5 mb above 100 GeV/c, roughly 10% of the pp total cross section. This behavior is shown in Fig. 1, taken from Baldini et al. [1]. As the energy increases, the three–body ΛpK^+ final state represents a smaller and smaller part of the total Λ production. For instance, we have

$$\frac{\sigma\left(pp \rightarrow \Lambda pK^+\right)}{\sigma\left(pp \rightarrow \Lambda X\right)} \approx \begin{cases} 0.04 & (12 \text{ GeV/c}) \\ 0.02 & (24 \text{ GeV/c}) \end{cases} \tag{1}$$

The three–body $K^+\Lambda p$ and $K^+\Sigma N$ final states are of particular interest, since one can make a reasonable attempt to calculate these cross sections theoretically. The data on these processes [2,3] in the few GeV region are displayed in Figs. 2 and 3. In this medium energy regime, it is still reasonable to describe the reaction mechanism in terms of meson exchanges, as depicted in Fig. 4. Calculations of this type have been carried out by Laget [2] and Deloff [4]; the latter results are questionable, since a fit is only obtained with $g^2_{KN\Lambda} \ll g^2_{KN\Sigma}$, whereas there are numerous indications from other data that the $KN\Lambda$ coupling constant $g_{KN\Lambda}$ is much stronger than that for $g_{KN\Sigma}$. For instance, from analyses of $\overline{K}N$ disperson relations, Baillon et al. [5] give $g^2_{KN\Lambda} = 0.8 \pm 3.2$, $g^2_{KN\Sigma} = 21.3 \pm 3.7$. A somewhat larger ratio of Σ/Λ couplings was extracted from data on Λ and Σ production in K^-p interactions [6]. Laget [2] uses reasonable coupling constants $g^2_{KN\Sigma} = 1$, $g^2_{KN\Lambda} = 14$, in agreement with values obtained from studies of hyperon–nucleon scattering [7] and kaon photoproduction reactions [8].

The Saturne data [3] shown in Fig. 3 display characteristic enhancements just above the Λp and ΣN thresholds at an invariant mass of $W = 2.053$ GeV/c^2 and 2.131 GeV/c^2, respectively. This is due to the strong s–wave YN attraction, i.e. the final state interaction amplitude t in Fig. 4. The pion exchange graph dominates the $pp \rightarrow K^+\Sigma N$ reactions (see Fig. 2), but the kaon exchange mechanism is more important for the $K^+\Lambda p$ channel. The direct kaon emission graph (bottom of Fig. 4) plays a key rôle in reproducing the structure which appears at the ΣN threshold, which also depends sensitively on the strong coupling of the Λp and ΣN channels.

Note that the relative phase between the π and K exchange amplitudes is not fixed à priori. Laget [2] has chosen the sign which gives the maximum additive effect on the cross sections. Further data, particularly on spin observables, are needed in order to check this relative phase and also other dynamical aspects of the model (the diagonal and non–diagonal $YN \rightarrow Y'N$ couplings, for instance). Such data could be obtained with high luminosity proton beams. Some predictions for spin observables are shown in the bottom half of Fig. 3.
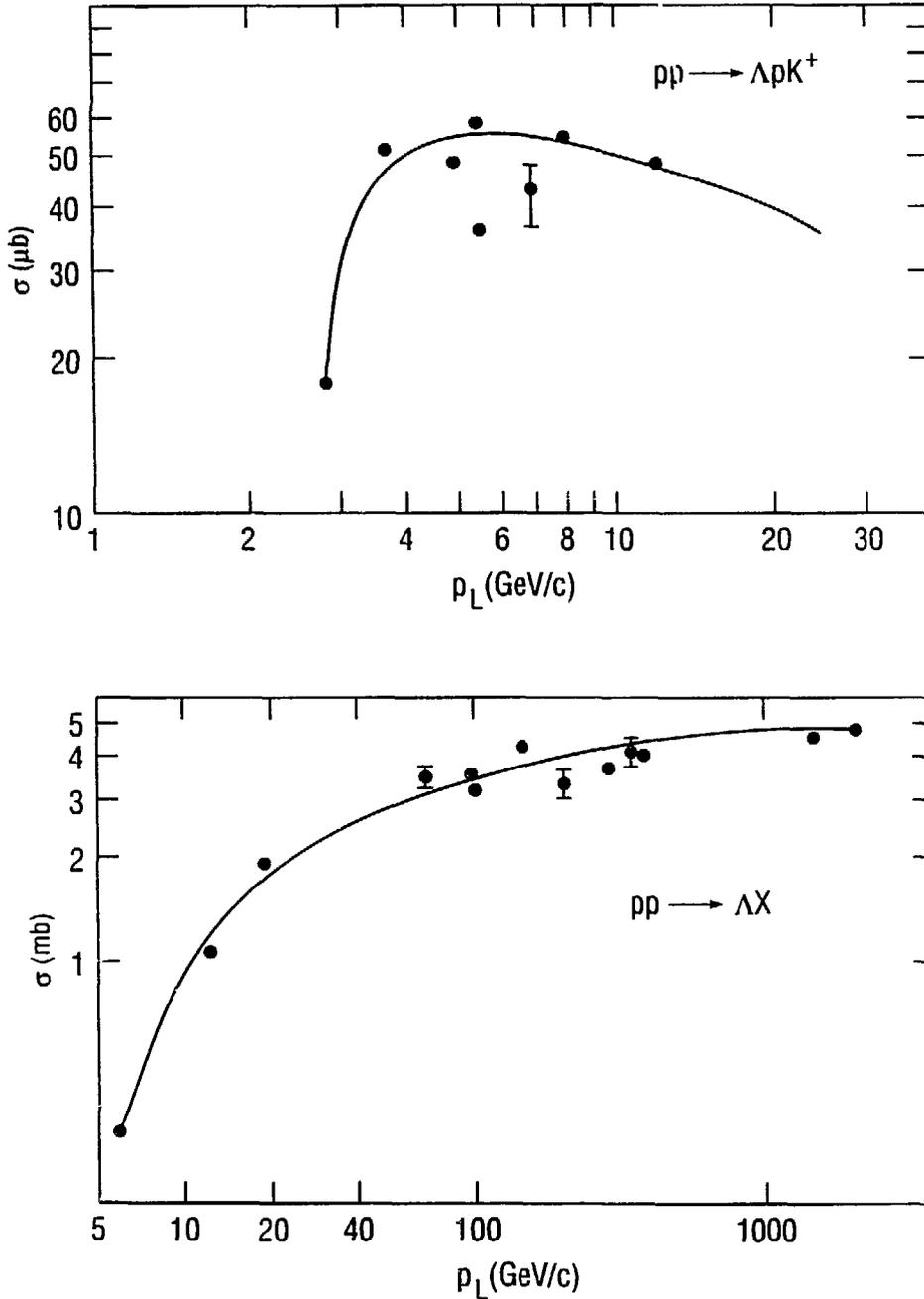
Figure 1: Total cross sections for inclusive Λ production and the three-body final state ΛpK^+ in pp collisions, as a function of lab momentum p_L, from Baldini *et al.* [1]. A few typical error bars are shown; the solid curves represent numerical fits to the data.

The meson exchange picture with $K\Lambda N - K\Sigma N$ coupled channels certainly makes sense in the region near threshold. As we pass to higher energies, one might ask where such a
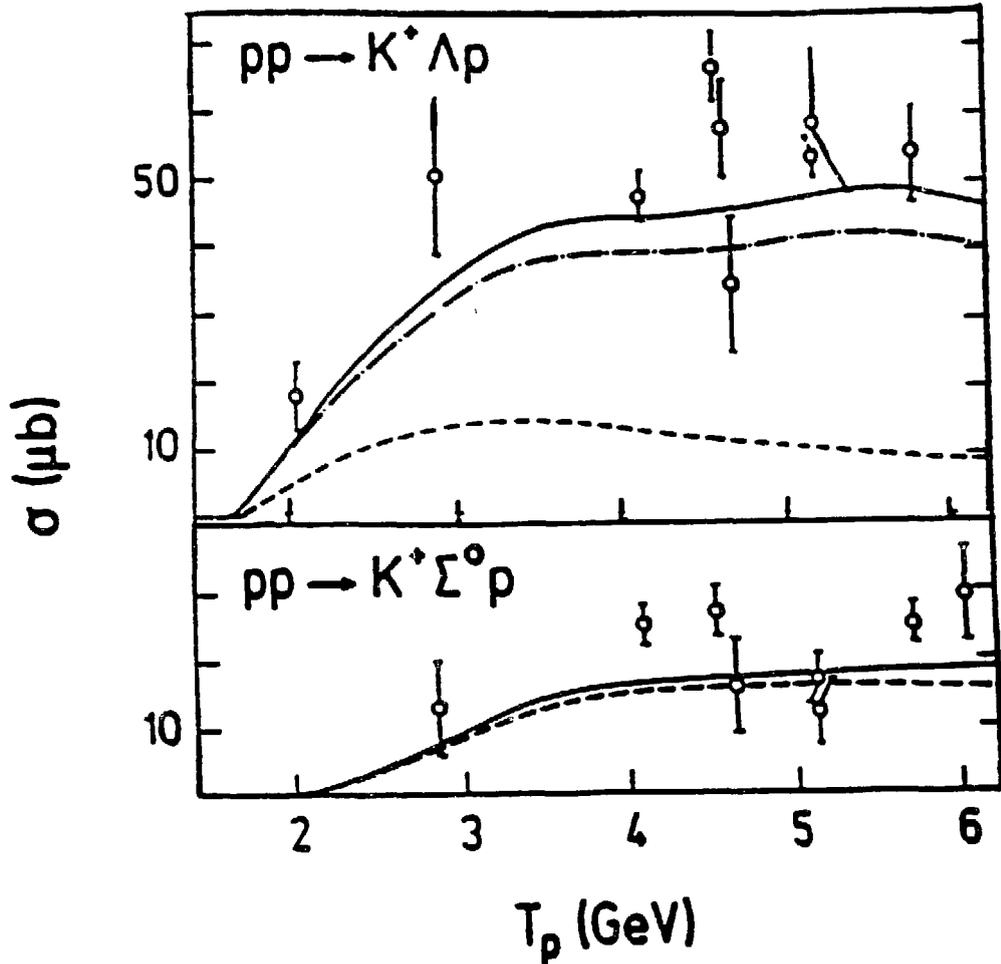
Figure 2: Total cross sections for the reactions $pp \to \Lambda pK^+$ and $\Sigma^0 pK^+$, as a function of proton lab kinetic energy in T_p. The dashed line represents the contribution of the pion exchange graph (see Fig. 4), while the solid and dash–dot lines include kaon exchange with two different values of the cutoff mass in the form factor for the meson–baryon vertex; from Laget [2].

picture breaks down, since many other reaction channels open up. The thresholds for some of these are given in Table 1.

Even though many other channels come into play above 3 GeV/c, the simple meson exchange picture works well at least up to $T_p = 6$ GeV, as shown in Fig. 2. A key ingredient in this success is the proper treatment of the energy dependence of the elastic $\Lambda N \to \Lambda N$ and $\Sigma N \to \Sigma N$ t-matrices which appear in Fig. 4. Although many channels may be energetically accessible, their effect appears only as an absorptive correction, i.e. channels
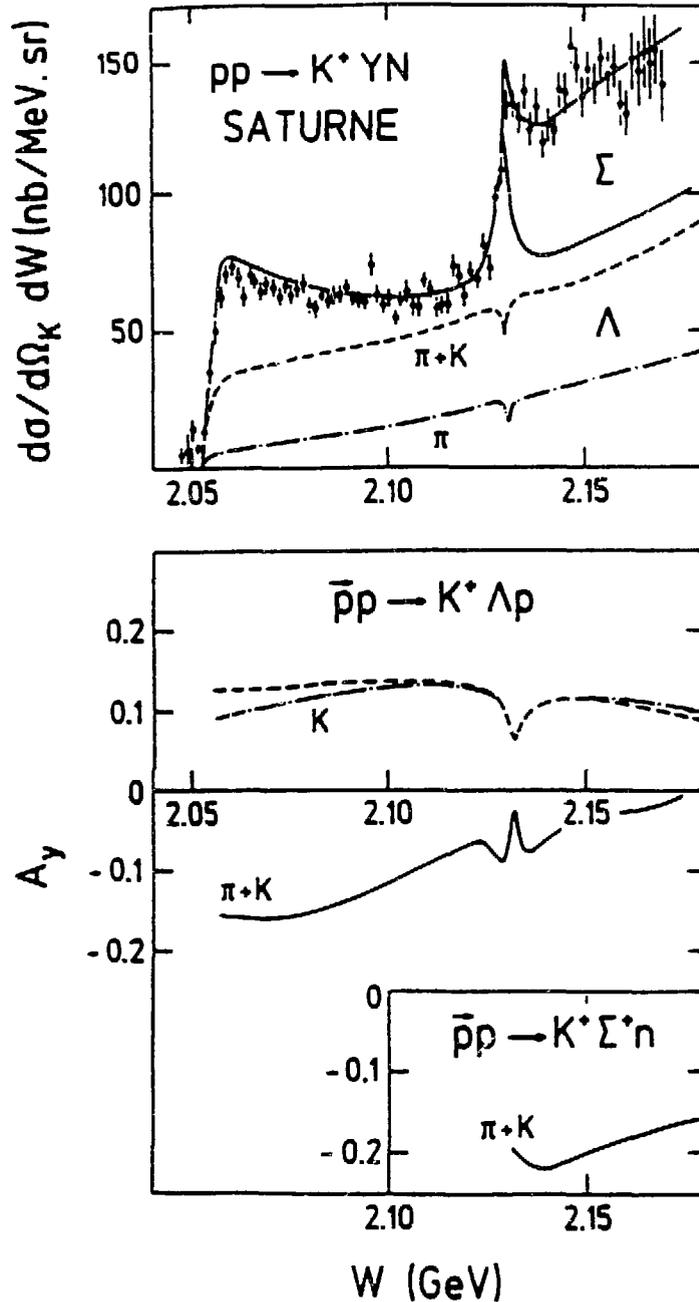
Figure 3: Top: Missing mass spectrum for the $pp \rightarrow K^+YN$ reaction at $T_p = 2.3$ GeV. The K^+ is measured at an angle $\theta_K = 10°$, and W is the invariant mass of the recoiling YN system. The data are from Frascaria *et al.* [3] and the theoretical curves are from Laget [2]. Various meson exchange contributions are indicated; the solid curve includes direct kaon emission. Bottom: Predictions [2] for the beam asymmetry A_y at 2.3 GeV. The solid curve represents the full calculation, including both pion and kaon exchange. The scale is the invariant mass W of the hyperon-nucleon system.
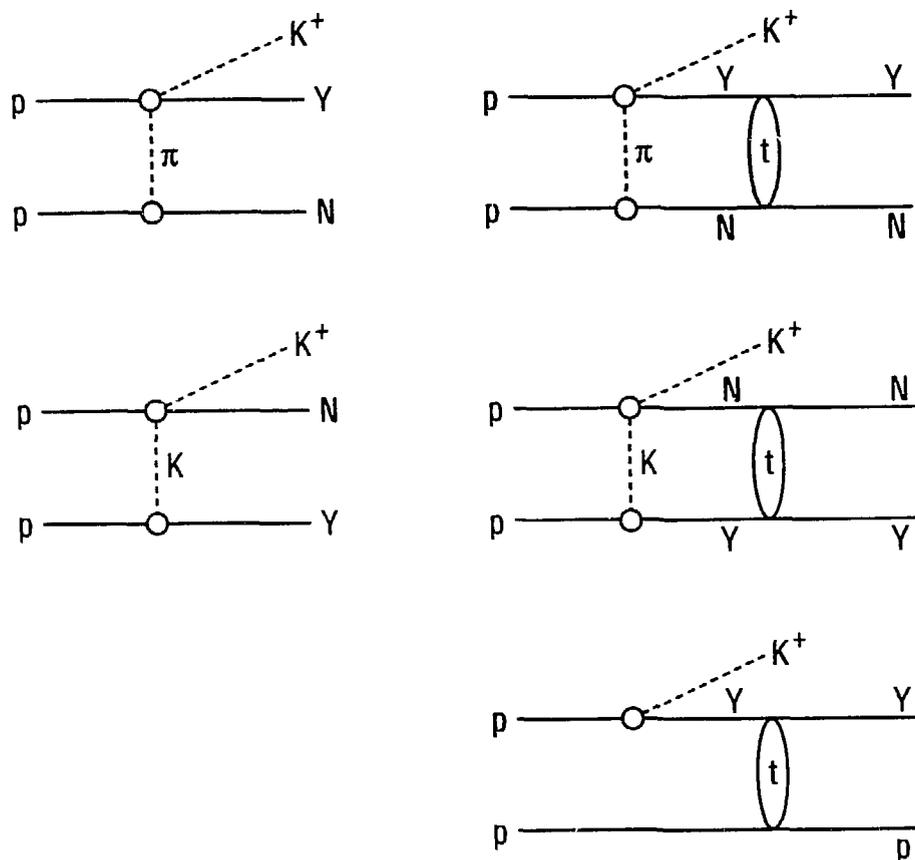
Figure 4: Meson exchange processes which contribute to the $pp \to YNK^+$ reaction. The oval labeled t stands for the YN scattering amplitude. The bottom graph represents the "direct" kaon emission, which represents a substantial contribution (see Fig. 3).

like $YN \to YN\pi$ are included in terms of the inelasticities η of the elastic partial wave amplitudes.

The further study of the $pp \to K^+ YN$ reactions, in particular the spin observables, is well worthwhile. Such experiments have been proposed at SATURNE and COSY. The spin information would provide strong constraints for theoretical models.

Table 1: Threshold lab momenta p_L and lab kinetic energy T_p for various final channels produced in pp collisions.

Channel	p_L (GeV/c)	T_p (GeV)
$\Lambda K^+ p$	2.34	1.582
$\Sigma^0 K^+ p$	2.57	1.794
$\Lambda K^+ p\pi^0$	2.74	1.958
$\Sigma^0 K^+ p\pi^0$	2.97	2.174
$\Sigma^0(1385) K^+ p$	3.15	2.35
$\Lambda(1405) K^+ p$	3.22	2.413
$\Lambda K^+ \Delta(1232)$	3.24	2.436

3. Hyperon–Nucleon Scattering: Spin Observables and SU(3)

The $pp \rightarrow K^+YX$ reaction, with K^+ detection for tagging, leads to the production of hyperons Y, which can then be scattered from a secondary proton or nuclear target, in order to study the YN interaction. In this section, we indicate the physics justification for such a program.

The existing information on hyperon–nucleon scattering is very sparse. Essentially all the low–lying total cross section data is collected in Fig. 5, taken from [9]. Compared to the NN data, the error bars for YN are rather large, and data exist only in a limited momentum range. There are also data on differential cross sections. Even at low momenta (160–170 MeV/c), the angular distributions are not isotropic, indicating a significant p–wave contribution.

The solid curves in Fig. 5 correspond to best fits in a meson exchange model for baryon–baryon scattering. The particular model shown here, due to the Nijmegen group [7], employs the exchange of nonets of mesons, namely

$$\{\pi, \eta, \eta'\}_{0-}, \quad \{\delta, \sigma, \mathcal{3}^*\}_{0+}, \quad \{\rho, \omega, \phi\}_{1-} \tag{2}$$

with a hard core cutoff at short distances. A more recent Nijmegen potential model, due to Maessen *et al.* [10], uses soft core form factors. Similar models have recently been developed by the Bonn group [11].

In the Nijmegen models [7,10], SU(3) symmetry is used to relate the coupling constants for hyperons and nucleons. For example, the coupling constants for the pseudoscalar octet $\{\pi, \eta_8, K\}$ are given by

$$g_{NN\eta_8} = (4\alpha_{PS} - 1)/\sqrt{3}, \quad g_{\Lambda NK} = -\frac{(1 + 2\alpha_{PS})}{\sqrt{3}}, \quad g_{\Sigma NK} = 1 - 2\alpha_{PS},$$

$$g_{\Sigma\Sigma\pi} = 2\alpha_{PS}, \quad g_{\Sigma\Lambda\pi} = g_{\Sigma\Sigma\eta_8} = -g_{\Lambda\Lambda\eta_8} = \frac{2(1 - \alpha_{PS})}{\sqrt{3}} \tag{3}$$
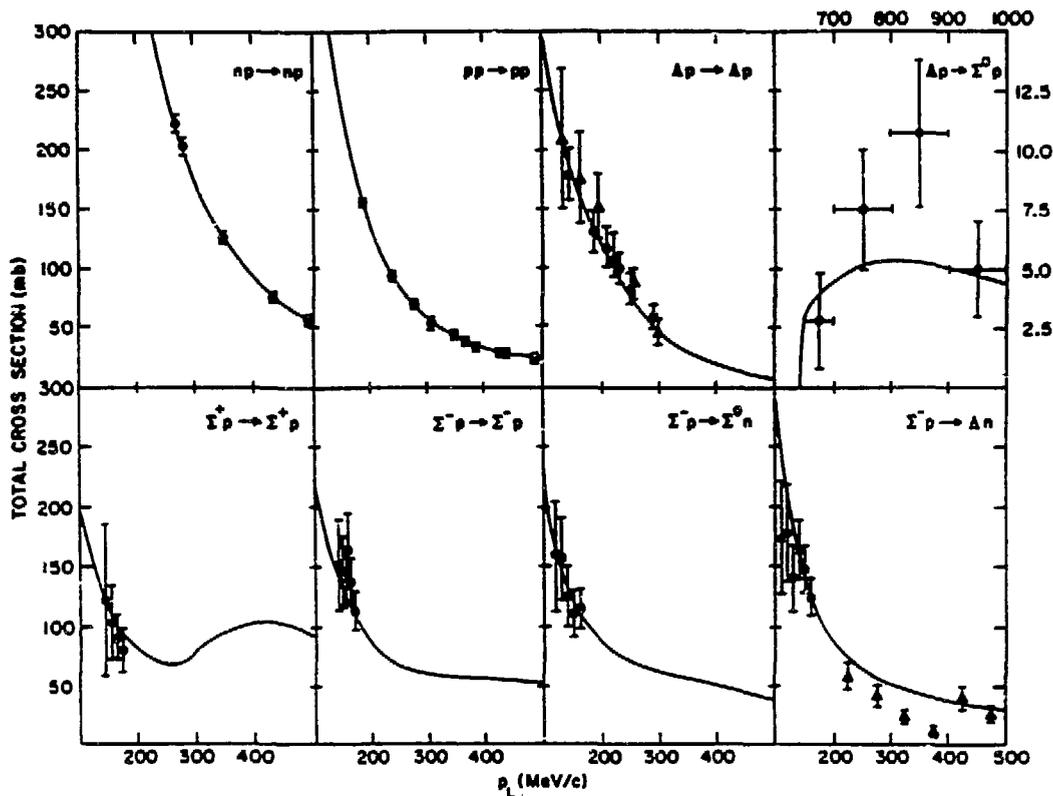
Figure 5: Total cross sections for NN and YN scattering, as a function of lab momentum p_L, from Ref. 9. The solid curves are potential model fits of the Nijmegen group (Model D, ref. [7]).

in units of $g_{NN\pi}$, where α_{PS} is the pseudoscalar F/D ratio. An angle θ_{PS} describes the octet (η_8)–singlet (η_1) mixing. In the Nijmegen models, α_{PS} is adjusted to achieve a best fit to the data ($\alpha_{PS} = 0.485$ in [7]; $\alpha_{PS} = 0.355$ in [10]). In the Bonn model [11], the SU(6) value $\alpha_{PS} = 2/5$ is picked. A unique α_{PS} cannot be determined from the baryon-baryon data, since its optimum value is intertwined with the parametrization of the short range potential. In SU(6), we predict the ratio

$$\frac{g^2_{\Sigma NK}}{g^2_{\Lambda NK}} = \frac{1}{27} \tag{4}$$

This very strong suppression of the ΣNK vertex is not seen in various production experiments, where Σ/Λ ratios of order $1/2$ are measured [6]. These larger ratios can be accommodated in SU(3) with a choice $\alpha_{PS} \simeq 0.3$, but are at odds with SU(6). Thus the imposition of an SU(6) constraint on meson–baryon couplings does not appear well motivated, even though one can achieve a good fit by using a flexible multi–parameter form for the short range cutoffs.

The fits to baryon–baryon scattering are driven by the high precision NN data. The YN data by themselves can be reproduced with a wide range of models, including simple one or two term separable potentials, which have no theoretical motivation. From the data of Fig. 5, we note that the charge exchange cross sections ($\Sigma^- p \rightarrow \Sigma^0 n$, Λn), which require isovector meson exchange, are of the same order as $\Sigma^- p$ or $\Sigma^+ p$ elastic scattering. Thus it is clear from the data that the ΣN potential must have a strong isospin ($\vec{t}_\Sigma \cdot \vec{\tau}_N$) dependence, which is naturally generated by π and ρ exchange. The degree of spin dependence is not so clear, since only spin averaged cross sections have been measured. In fact, the various models predict quite different spin dependences. For instance, Nijmegen Models D and F have

$$a\left({}^1S_0\right) \approx a\left({}^3S_1\right) \tag{5}$$

for the ΛN singlet and triplet scattering lengths, whereas the soft core model [10] suggests a significant spin dependence:

$$a\left({}^1S_0\right) \simeq -2.8 \text{ fm}, \quad a\left({}^3S_1\right) \simeq -1.4 \text{ fm} \tag{6}$$

Further, the models predict a strong spin dependence for ΣN reactions. For instance, Models D, F [7] at low energies lead to

$${}^3S_1 \text{ dominance for } \Sigma^- p \rightarrow \Sigma^- p, \ \Lambda n$$
$${}^1S_0 \text{ dominance for } \Sigma^+ p \rightarrow \Sigma^+ p \tag{7}$$

Different models which give equivalent fits to spin–averaged cross sections predict significantly different spin separated cross sections $\sigma_0({}^1S_0)$ and $\sigma_1({}^3S_1)$. Thus the main motivation of future experiments on YN scattering is to measure spin observables. The simplest of these is the elastic polarization $P(\theta)$, which is sensitive to the baryon–baryon spin–orbit couplings. Note that for YN interactions, there exist both symmetric $[(\vec{\sigma}_Y + \vec{\sigma}_N) \cdot \vec{L}]$ and antisymmetric $[(\vec{\sigma}_Y - \vec{\sigma}_N) \cdot \vec{L}]$ spin–orbit terms, whereas for the NN system the antisymmetric coupling drops out because of the requirements of the Pauli principle. From Λ–hypernuclear spectra, there is evidence [12] that the one–body Λ–nucleus spin–orbit strength V_{LS}^Λ is very small compared to the value V_{LS}^N for a nucleon. Polarization data on Λp scattering would be invaluable in clarifying the relation between the two–body ΛN and many–body Λ–nucleus spin–orbit potentials. With respect to experiments with protons in the few GeV region, some questions to consider are: i) Can we make use of the polarization of the Λ's from the primary $pp \rightarrow K^+ \Lambda p$ reaction?; ii) Is it necessary to tag Λ production by detecting the K^+?; iii) What are the virtues/disadvantages of a polarized proton target for Λp studies?.

Another issue pertaining to hyperon–nucleon scattering studies is the degree to which SU(3) symmetry is broken. In the SU(3) limit, we can write the baryon–baryon scattering amplitude as

$$T = a + b F^2 + c G^3 \tag{8}$$

in terms of the quadratic (F^2) and cubic (G^3) Casimir operators of SU(3). Here $\{a, b, c\}$ are functions of spin, energy and momentum transfer. An amplitude of the form [8] implies the following cross section relations [9]:

$$\sigma_0 \left(\Sigma^+ p \to \Sigma^+ p\right) = \sigma_0 \left(np \to np\right) \tag{9a}$$

$$\sigma_0 \left(\Sigma^- p \to \Lambda n\right) = \frac{1}{3} \sigma_0 \left(\Sigma^- p \to \Sigma^0 n\right) \tag{9b}$$

$$\sigma_0 \left(\Lambda p \to \Lambda p\right) = \frac{1}{6} \left[5\sigma_0 \left(\Sigma^+ p \to \Sigma^+ p\right) + \sigma_0 \left(\Sigma^- p \to \Sigma^- p\right) - \frac{5}{3} \sigma_0 \left(\Sigma^- p \to \Sigma^0 n\right) \right] \tag{9c}$$

$$\sigma_1 \left(\Lambda p \to \Lambda p\right) = \frac{1}{2} \left[3\sigma_1 \left(\Sigma^- p \to \Sigma^- p\right) + 3\sigma_1 \left(\Sigma^- p \to \Sigma^0 n\right) - \sigma_1 \left(\Sigma^+ p \to \Sigma^+ p\right) \right] \tag{9d}$$

It is understood that these relations apply after differences in kinematical phase space factors are removed [9]. In potential models, SU(3) is broken not only by baryon mass differences, but also by those of the exchanged mesons. Since the π, η and K masses are very different, one might expect SU(3) breaking effects to be huge. However, the SU(3) relations are predicted [9] to be satisfied at the 30% level in the Nijmegen potential model.

In order to verify the SU(3) relations of Eq. (9), spin separated cross sections $\sigma_{0,1}$ are required. This provides motivation for ΛN and ΣN scattering experiments with polarized hyperon beams or a polarized hydrogen target (or both).

4. Production of Hypernuclei with Proton Beams

Most hypernuclear research has been done with kaon (K^-) and pion (π^+) beams [12]. Some of the basic reactions for Λ and Σ production are

$$K^- n \to \pi^- \Lambda \tag{10a}$$

$$\pi^+ n \to K^+ \Lambda \tag{10b}$$

$$K^- p \to \pi^+ \Sigma^- \tag{10c}$$

The process (10a) involves small momentum transfer q at small angles, so a slow Λ is produced which readily sticks to a nuclear core, yielding a bound hypernucleus $_\Lambda$A. Reaction (10b) involves $q \geq p_F$, even at small angles, and thus tends to populate hypernuclear states of the highest available spin [13]. The reaction (10c) produces Σ hyperons, which also experience attractive forces capable of binding them to a nuclear core. Due to the strong conversion $\Sigma N \to \Lambda N$, Σ states are generally expected to be broad, although specific mechanisms have been proposed which may suppress their width to values $\Gamma \leq 5$

MeV, where they become observable as quasiparticle excitations [14]. The existence of Σ hypernuclei remains controversial.

Progress in hypernuclear structure physics requires experiments of much higher energy resolution than currently available ($\Delta E \simeq 3 - 5$ MeV). Such experiments are eventually planned at CEBAF, where the process

$$\gamma p \rightarrow K^+ \Lambda \tag{11}$$

will be used with virtual or real photons. The kinematics of the electroproduction reaction (11) is similar to (10b), but (γ, K^+) has a large spin flip amplitude, whereas (π^+, K^+) does not (at small angles). Thus different hypernuclear states are preferentially populated in (γ, K^+) and (π^+, K^+) reactions; see [15] for a detailed discussion. Future prospects for high resolution hypernuclear structure studies have been discussed at a previous workshop [16].

Meson or photon beams are the method of choice for exploring the properties of hypernuclei, but it is also possible to produce hyperfragments with proton beams, and this method merits further study. The basic process is $pN \rightarrow K\Lambda N$, followed by the sticking of the Λ or ΛN to a nuclear fragment. Reactions to consider are

$$p + A_Z \rightarrow {}_\Lambda A'_{Z'} + X \tag{12a}$$

$$p + A_Z \rightarrow K^+ + p' + {}_\Lambda A_{Z-1} \tag{12b}$$

$$p + A_Z \rightarrow K^+ + {}_\Lambda (A+1)_Z \tag{12c}$$

Since the Λ is generally produced with a sizeable momentum in the lab frame, the sticking probability is always small. In (12a), the hypernucleus is detected through the weak decay $\Lambda \rightarrow p\pi^-$. The experimental data on hypernuclear yields in pA and $\pi^- A$ collisions have been reviewed by Lyukov [17]. Some results are shown in Fig. 6. The yield of hyperfragments in pA interactions does not exceed 2×10^{-3} or so, with a broad maximum centered around 50 GeV/c. The frequency of observed mesonic decays is an order of magnitude smaller ($1 - 3 \times 10^{-4}$ from 10–50 GeV/c). The charge distribution of observed hyperfragments is centered around $Z = 2$, and decreases rapidly for $Z > 3$. Thus only rather light fragments are observed by this method; in heavier hypernuclei, the dominant weak decay mode is non–mesonic ($\Lambda N \rightarrow NN$), since the $\Lambda \rightarrow p\pi^-$ mode is Pauli blocked.

The solid curves in Fig. 6 represent theoretical expectations based on a simple coalescence model [17], in which the bound hypernucleus is formed only when the Λ is produced with a small momentum relative to the nuclear core. Although the coalescence picture leads to the correct order of magnitude for the hyperfragment yield, the existing data are not precise enough to test the detailed form of the predicted energy dependence.

The reactions (12b) and (12c) involve a large momentum transfer (defined as $p_L - p_{K^+}$ for a K^+ at $0°$). The three–body final state of (12b) will have a larger cross section than that for the two–body channel (12c), since the momentum transfer is shared between the
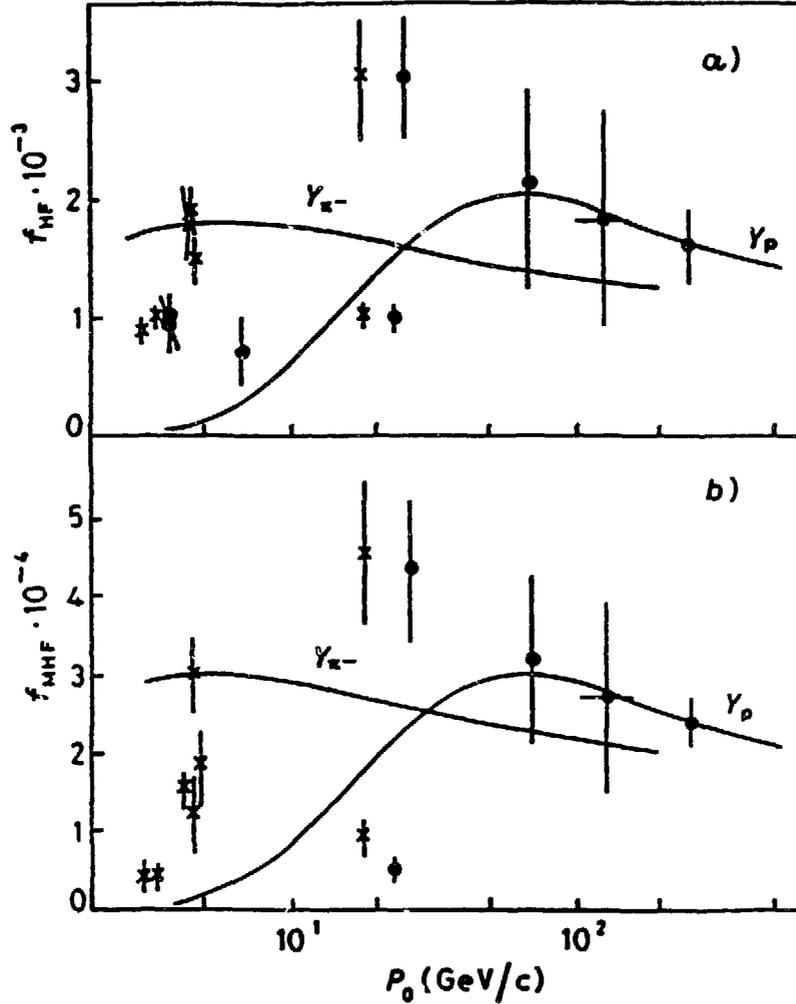
Figure 6: In a) we show the measured yields f_{HF} in units of 10^{-3}, for hyperfragments obtained in π^- or p–nucleus collisions, as a function of the incident particle momentum P_0. Theoretical expectations are shown as the solid curves Y_{π^-} and Y_p. Circles refer to pA and crosses to $\pi^- A$ interactions. In b), we indicate the frequency of observation f_{MHF} (in units 10^{-4}) of mesic decays ($\Lambda \rightarrow p\pi^-$) of hyperfragments. The plot is taken from Lyukov [17].

K^+ and p'. However, in (12b), one must detect both the K^+ and p' in order to construct the missing mass spectrum for the hypernucleus, so the advantage in cross section is lost. Recently, there have been experiments at Saturne, due to Boivin et al. [18], to search for the two–body reactions

$$p + {}^3\text{He} \rightarrow K^+ + {}^4_\Lambda\text{He} \tag{13a}$$

$$p + {}^4\text{He} \rightarrow K^+ + {}^5_\Lambda\text{He} \tag{13b}$$

at a proton kinetic energy of 2.1 GeV and a kaon lab angle $\theta_{K+} = 7°$. The momentum transfer here is about 500 MeV/c and the missing mass resolution is 1.5 MeV. From other data, $^4_\Lambda$He is known to have a 0^+ ground state and a bound 1^+ excited state at 1.1 MeV; $^5_\Lambda$He has a single $1/2^+$ bound state. No clear signal of bound state formation was observed, leading to upper limits

$$\left(\frac{d\sigma}{d\Omega_L}\right)_{7°} < \begin{cases} 3 \text{ nb/sr} & \text{for (13a)} \\ 1.7 \text{ nb/sr} & \text{for (13b)} \end{cases} \tag{14}$$

The observed limits (14) are within the range of theoretical estimates [19,20]. Because the momentum transfer is large, the rôle of short range correlations is extremely important. Such correlations enhance the high momentum components in the single particle momentum distribution of the target nucleus, and greatly increase the cross section above the value obtained with uncorrelated Gaussian wave functions. With correlations, Shinmura [19] predicts $\sim$ 2 nb/sr for reaction (13b) at small angles, comparable to the observed limits (14). This prediction is very model dependent, however.

The message here is the following: the (p, K^+) reaction is a good probe of the reaction mechanism for hypernuclear production in high momentum transfer processes. However, the cross sections are very small ($\lesssim$ 1–2 nb/sr) near 2 GeV and one is unlikely to attain a sufficiently high energy resolution to perform detailed spectroscopic studies. A more promising direction of research is the study of the strangeness production mechanism itself in proton–nucleus collisions. Some data [21,22] at 10 GeV indicate that the production of high energy K^+ and K^- mesons in pA collisions is described by the same structure function f of the nucleus as the production of other particles. This universality, observed for K^- mesons which consist only of sea quarks ($s\bar{u}$), may indicate [22] that the nucleus contains a hard quark–antiquark sea differing from the soft sea present in the nucleon.

5. Hypernuclear Physics with Pion Beams: Polarization Phenomena

The (π^+, K^+) reaction on nuclear targets has enormous potential for studies of hypernuclear structure [12,13,16]. Pion beams near 1 GeV/c are optimal, with a premium on intensity for high resolution studies. In the momentum range 1–1.2 GeV/c, we straddle the peak of the cross section for the elementary process $\pi^+ n \rightarrow K^+ \Lambda$, by which a neutron is converted into a Λ hyperon, which can then bind to a nuclear core to produce a hypernucleus of strangeness $S = -1$. The formation of the hypernucleus is tagged by the detection of the strange K^+ meson. A high π^+ intensity would enable us to perform coincidence experiments involving strong, electromagnetic or weak decays of various hypernuclear states. Since the (π^+, K^+) reaction at finite angles can produce significant hypernuclear polarization, weak decay studies would further elucidate the properties of

the nucleon–catalyzed Λ weak decay amplitudes, i.e. $\Lambda N \to N N$. Studies of γ decays of hypernuclear excited states provide us with precise information on the spin dependence of the effective lambda–nucleon (ΛN) interaction in the nuclear medium. High energy resolution (π^+, K^+) experiments (~ 200 keV resolution is desirable) can directly resolve the fine structure of the hypernuclear spectrum in favorable cases. Thus far only coarse resolution (typically 3 MeV) hypernuclear experiments have been possible. The first (π^+, K^+) experiments at the Brookhaven AGS and KEK [23] have served to clarify the single particle properties of the Λ, i.e., the properties of the Λ–nucleus mean field [24]. To approach the level of precision of non–strange nuclear spectroscopy, a high resolution capability is clearly necessary.

At non-zero angles, the (π^+, K^+) reaction can be used to produce *polarized* hypernuclei. [25-27] In the elementary pseudoscalar meson-baryon process, the amplitude t and the Λ polarization P_Λ are of the form

$$t = f + ig\vec{\sigma} \cdot \hat{n}$$
$$P_\Lambda = 2Im\left(fg^*\right) / \left(|f|^2 + |g|^2\right) \tag{15}$$

where $\vec{\sigma}$ is the baryon spin and $\hat{n}$ is the normal to the scattering plane. In the regime of $p_\pi \approx 1 - 1.1$ GeV/c, P_Λ is quite substantial for $\theta_L \geq 5°$. This offers the attractive possibility of producing polarized hypernuclear states. As we shall see, the polarization varies in an interesting way, depending on the quantum numbers of the initial and final states. There is also an interplay between two sources of hypernuclear polarization [26], namely the f-g interference in the elementary amplitude and the effects of meson distortion in the medium, i.e., the difference between the absorption experienced by mesons passing on the near-side or far-side of the nucleus.

Consider a transition $J_i M_i \to J_f M_f$, induced by the (π^+, K^+) reaction. The matrix element is

$$M\left(J_i M_i; J_f M_f\right) = \left\langle J_f M_f \left| \int d^3 r \chi^{(-)*}\left(\vec{p}_K, \vec{r}\right) \chi^{(+)}\left(\vec{p}_\pi, \vec{r}\right) \right.\right.$$
$$\left.\left. \sum_{k=1}^{A} U_-\left(k\right) \delta^{(3)}\left(\vec{r} - \vec{r}_k\right)\left[f + ig\vec{\sigma}_k \cdot \hat{n}\right] \right| J_i M_i \right\rangle \tag{16}$$

where $\chi^{(\pm)}$ are meson distorted waves, and U_- is the U–spin lowering operator which generates the $n \to \Lambda$ transition. The cross section is proportional to $\sum_{M_f} |M(M_f)|^2$, while the polarization P_f of the hypernuclear state $|J_f\rangle$ is defined as

$$P_f = \frac{1}{J_f} \sum_{M_f} M_f P\left(M_f\right)$$
$$P\left(M_f\right) = \sum_{M_i} |M\left(J_i M_i; J_f M_f\right)|^2 / \sum_{M_i, M_f} |M\left(J_i M_i; J_f M_f\right)|^2 \tag{17}$$

The polarization P_f is a measure of the population asymmetry with respect to the reaction plane.

For the special case of a $J_i = 0$ target and a pure particle-hole hypernuclear state, the polarization assumes a simple analytic form. For example, consider the configurations in $^{12}_\Lambda C$:

$$\left[\Lambda S_{1/2} \otimes {}_n P^{-1}_{3/2}\right]_{1^-,2^-}$$
$$\left[\Lambda P_{3/2} \otimes {}_n P^{-1}_{3/2}\right]_{0^+,1^+_1,2^+_1,3^+} \tag{18}$$
$$\left[\Lambda P_{1/2} \otimes {}_n P^{-1}_{3/2}\right]_{1^+_2,2^+_2}$$

For the 1^- ground state of $^{12}_\Lambda C$, we have

$$P_{1^-} = (P_{PW} + P_A)/(1 + P_{PW} P_A)$$
$$P_{PW} = -4\operatorname{Im}[fg^*]/(4|f|^2 + |g|^2) \tag{19}$$
$$P_A = -2\sqrt{2}\operatorname{Im}[I^*(0) I(1)]/(|I(0)|^2 + 2|I(1)|^2)$$

where

$$I(m) = \langle \phi_\Lambda \| \tilde{j}_{1m} \| \phi_n \rangle \tag{20}$$

and $\tilde{j}_{1m}$ is obtained by expanding the product $\chi^{(-)}\chi^{(+)}$ in partial waves [26]; in PWA, $\tilde{j}_{1m}$ reduces to $j_1(qr)\delta_{mo}$, and $P_{1^-} = P_{PW}$. Meson absorption effects provide the physical origin of P_A. In most cases, particularly for $\theta_L \le 15°$, the influence of P_A is relatively minor, and we have $P \approx P_{PW}$. In plane wave approximation (PWA), one obtains simple analytic formulae for the polarization. For instance, for the 1^- ground state of $^{12}_\Lambda C$, we have

$$P_{1^-} = -4\operatorname{Im}[fg^*]/(4|f|^2 + |g|^2) \approx -\frac{P_\Lambda}{2} \tag{21}$$

for small θ_L, since here $|g|^2 \ll |f|^2$. The cross sections for the unnatural parity states peak in the vicinity of $\theta_L \approx 15°$, at the 0.5 – 1 $\mu b/sr$ level for 2^- and 3^+. In this angular region, the 1^- and 2^+ cross sections have dropped to the 5 $\mu b/sr$ level, so a high resolution experiment could probably separate the 3^+ and 2^+ levels, thus providing information on the spin dependence of the ΛN interaction.

The polarization expected for unnatural parity states is negligible. However, for the natural parity 1^- and 2^+_2 states, P is very substantial near $\theta_L = 15°$, where the cross section is still large enough to be measurable. When configuration mixing of the 2^+_1 and 2^+_2 states is included, the polarization pattern could be strongly modified. Thus polarization measurements offer another promising spectroscopic tool for pinning down the ΛN interaction.

Ejiri *et al.* [25,27] have shown that polarized hypernuclear states may be populated through nucleon and γ decays of highly excited compound systems. Polarized hypernuclei

are particularly useful when combined with coincidence measurements of decay particles. For instance, the asymmetry of weak decay pions [28] provides information on hypernuclear structure and pion distortions inside the nucleus. A polarized hypernucleus could also be used to obtain a measurement of the Λ magnetic moment in a hypernucleus. Finally, we note that the angular distribution of nucleons from the non-mesonic weak decay of a polarized hypernucleus reveals interference terms between parity-conserving and parity-violating weak amplitudes.

If a polarized hypernucleus decays, the angular distribution of the nucleon has the form

$$W(\theta) = A_0 + A_1 P_\Lambda P_1(\cos\theta) \tag{22}$$

where P_Λ is the polarization of the Λ and A_1 is given by an interference of parity–conserving $^3S_1 \rightarrow {}^3S_1 - {}^3D_1$ and parity–violating $^3S_1 \rightarrow {}^3P_1$ amplitudes for the $\Lambda N \rightarrow NN$ weak process. The first measurements of such weak decay angular distributions were recently performed at KEK by Ejiri and his collaborators [29]. Because of the rather coarse energy resolution, however, one cannot make detained comparisons with theoretical expectations.

6. Final Remarks

What contribution could a few GeV cooled proton facility make to strange particle physics? The key word in this discussion is SPIN. In the elementary production processes $pp \rightarrow K\Lambda N$, $K\Sigma N$, KY^*N, spin observables are crucial in probing the reaction mechanism. There are currently no spin data, although several proposals exist. The meson exchange approach, which rules at energies up to a few GeV, must break down at some point, to be supplanted by a picture involving explicit quark dynamics. If we study the secondary collisions of Λ or Σ hyperons produced in primary pp collisions, we can qualitatively improve our knowledge of YN scattering phenomena. To make progress, it is essential to measure the polarization P for ΛN and ΣN scattering, as well as the spin–separated cross sections $\sigma_{0,1}$. A closer look at spin observables in inclusive hyperon production is also warranted, as well as a global investigation of the strangeness production mechanism in proton–nucleus collisions. Finally, definitive measurements of cross sections for Λ hypernuclear production in pA interactions would provide useful tests of coalescence models (for inclusive $_\Lambda A$ production) or short range correlations in two–body reactions at high momentum transfer.

Acknowledgments

REFERENCES

1. Baldini *et al.*, Landolt–Börnstein New Series 1/12b, p. 162.
2. J.M. Laget, Phys. Lett. B259, 23 (1991).
3. R. Frascaria *et al.*, Nuoco Cim. 102A, 561 (1989).
4. A. Deloff, Nucl. Phys. A505, 583 (1989).
5. P. Baillon *et al.*, Phys. Lett. 50B, 383 (1974) and Nucl. Phys. B134, 31 (1978).
6. E. Hirsch, U. Karshon and H.J. Lipkin, Phys. Lett. 36B, 385 (1971).
7. M.M. Nagels, T.A. Rijken and J.J. deSwart, Phys. Rev. D15, 2547 (1977) and D20, 1633 (1979).
8. R.A. Adelseck and B. Saghai, Phys. Rev. C42, 108 (1990).
9. C.B. Dover and H. Feshbach, Ann. Phys. 198, 321 (1990).
10. P.M.M. Maessen, T.A. Rijken and J.J. deSwart, Phys. Rev. C40, 2226 (1989).
11. B. Holzenkamp, K. Holinde and J. Speth, Nucl. Phys. A500, 485 (1989).
12. R.E. Chrien and C.B. Dover, Ann. Rev. Nucl. Part. Sci. 39, 113 (1989).
13. C.B. Dover, L. Ludeking and G.E. Walker, Phys. Rev. C22, 2073 (1980).
14. C.B. Dover, D.J. Millener and A. Gal, Phys. Rep. 184, 1 (1989).
15. C.B. Dover and D.J. Millener, *Electroproduction of Strangeness*, in Modern Topics in Electron Scattering, Eds. B. Frois and I. Sick, World Scientific, Singapore (1991), pp. 608–44.
16. LAMPF Workshop on (π, K) Physics, AIP Conf. Proc. No. 224, Particles and Fields Series 43, Eds. B.F. Gibson *et al.*, American Inst. of Physics, New York (1991).
17. V.V. Lyukov, Nuovo Cim. 102A, 583 (1989).
18. M. Boivin *et al.*, *Upper Limits for Light Hypernuclei Production Rates in the (p, K^+) Reaction*, Saclay preprint (1991).
19. S. Shinmura, Nucl. Phys. A450, 147c (1986); Prog. Theor. Phys. 76, 157 (1986).
20. M.G. Huber, B.C. Metsch and H.G. Hopf, Lecture Notes in Physics, Vol. 242, p. 499, Springer (1986).
21. D. Armutliiski *et al.*, Sov. J. Nucl. Phys. 47, 473 (1988).
22. S.V. Boyarinov *et al.*, Sov. J. Nucl. Phys. 50, 996 (1989).
23. P.H. Pile *et al.*, Phys. Rev. Lett. 66, 2585 (1991).
24. D.J. Millener, C.B. Dover and A. Gal, Phys. Rev. C38, 2700 (1988).
25. H. Ejiri *et al.*, Phys. Rev. C36, 1435 (1987).
26. H. Bandō, T. Motoba, M. Sotona and J. Žofka, Phys. Rev. C39, 587 (1989).
27. T. Kishimoto, H. Ejiri and H. Bandō, Phys. Lett. B232, 24 (1989).
28. T. Motoba, K. Itonaga and H. Bandō, Nucl. Phys. A489, 683 (1988).
29. S. Ajimura *et al.*, Phys. Rev. Lett. 68, 2137 (1992) and Phys. Lett. 282B, 293 (1992).

SUMMARY OF HFBR IRRADIATIONS

11-01-92 TO 11-30-92

DATE	PROJECT/ORGANIZATION	HOURS	FACILITY	DESCRIPTION OF SAMPLE
11/02/92	NYSHD	5.733	V-11	CLOUD WATER
11/02/92	CHEMISTRY	0.083	V-14	Ca METAL
11/10/92	CHEMISTRY	16.567	V-12	LIMESTONE
11/12/92	MEDICAL	627.017	V-15	Sn-117 FLAKES
11/12/92	TENN. TECH. UNIV.	167.950	V-11	Ar-36
11/13/92	ARGONNE NAT. LAB.	402.833	V-16	MULTI-LAYER FILMS (cont. Nb,O,V,Al)

NO. OF IRRADIATION HOURS OR PARTIAL HOURS= 1223
NO. OF SAMPLE CAPSULES LOADED= 6

DISCLAIMER